Original Research Article

Application of UV-Visible Spectroscopy in Kinetic Study of Molybdate Complexation Reactions and Phosphate Content Quantitation

ABSTRACT

UV-visible spectroscopic measurements were used to characterize the formation of two ammonium-molybdate complexes, to elucidate its kinetics, and to carry out spectrophotometric quantitation of percent phosphate content in selected commercially available fertilizers. The kinetic study of ammonium-molybdate [$(NH_3)_6Mo_7O_{24}$] reaction with hydrazine (N_2H_2) yielding ammonium-hydrazine-molybdate complex (AHM) and that of reaction of AHM with phosphate $[PO_4]^{3-}$ to give phospho-ammonium-hydrazine-molybdate (AHPM) complex revealed that both proceed via zero-order kinetics (R^2= 0.99) with rate constants in the order of 10^{-5} and 10^{-4} M/s respectively. The kinetic experiments revealed that the rate of formation of the AHM complex is sensitive to an increase in N_2H_2 ligand concentration. For both reactions, the highest complexation rates were observed within the first 1000 s. Complex dissociation and association equilibria events were observed at extended reaction periods in the kinetic experiments. The AHPM system (containing complexed phosphates) used in spectrophotometric quantitation of phosphate levels in fertilizer samples was found to obey the *Beer-Lambert* equation in the visible region at λ max. = 820 nm within the concentration range of 5 – 90% phosphate content (R^2 = 0.99). Of the fertilizer randomized sampled from Nakuru Municipality in Kenya, and analyzed the percent phosphate content among the inorganic fertilizers was found to range between 61.7% - 82% with a mean of 72.86% +/- 6.98 SD. Whereas in the organic fertilizer samples investigated, it was found to range between 43.8 % - 58.2% with means of 52.55% +/- 6.77 SD. The organic fertilizers were found to have significantly lower phosphate levels based on an unpaired *t*-test revealing that the mean percent concentrations between the two groups of fertilizer samples tested are significantly different at 95% CI (*P* value < 0.05).

Keywords: Molybdate complex formation, Kinetics, Percent phosphate analysis, UV-Visible Spectroscopy

1. INTRODUCTION

Phosphates constitute one of the most important components in many commercial fertilizers that makes the elemental phosphorus (P) available as an essential nutrient that supports healthy plant growth and can increase crop yields. It is estimated that P deficiencies occur in nearly 67% of arable land designated for crop production worldwide.[1,2] The decline of the world's P-sources has prompted its conservation and management strategies to combat P-deficiency towards safeguarding food security.[1,3] Fertilizers play a vital role in protecting

crop health and guaranteeing quality food crop production. With an ever-rising global population that is increasingly facing challenges of food security, there has been a growing need to employ P-based fertilizers judiciously routinely test for the levels of phosphates for quality control and consumer assurance purposes.[4] To this end, simpler and less expensive analytical methods continue to be investigated.

Phosphorus can be made available via the salts of phosphates (PO_4^{3-}), monohydrogen phosphate (HPO_4^{2-}), and dihydrogen phosphate ($H_2PO_4^-$). These anions can readily interconvert, and the predominant species depends on the pH.[5] The chemistry of molybdenum blue complexes has in the past been exploited in the determination of P and phosphates with varied reaction conditions.[6,7,8] Some of these methods require expensive equipment, are complicated, laborious, and depend on elaborate extraction procedures subject to errors hence the need for the exploration and refinement of sensitive and reliable simple spectrophotometric techniques that can be applied in common laboratories for quick routine quantification of phosphates.[9] A number of these procedures involving spectrophotometric analysis rarely illustrate the relevant wavelength scan measurements and analysis of the kinetic data to support with depth the basis of the investigations.[9–12] In this study, we explore UV-Visible spectroscopic wavelength scan measurements and kinetic photometric experiments to characterize the formation of molybdenum complexes towards developing and validating a facile alternative variant method that can be applied in the rapid determination of percent phosphate content in fertilizers. The colorimetric method is based on the chemistry of the formation of a molybdate complex that forms intense blue coloration as it binds the phosphate ligand anions in the solution. The analyte peak is kinetically and spectroscopically elucidated. Finally, the validated method is used to quantify the percent phosphate content in selected commercially available inorganic and organic fertilizers.

2. MATERIALS AND METHODS

2.1 Experimentals

The chemicals used include ammonium molybdate, potassium dihydrogen phosphate, and hydrazine sulfate. All the chemicals were of analytical reagent grade as obtained from Kobian Scientific®, Kenya. Distilled water was also used in the dilutions.

2.1.1 Preparation of acidified ammonium molybdate and solution

Exactly 6.25 g of ammonium molybdate was accurately weighed and transferred onto a clean 100 mL volumetric flask. A solution of 10 N sulphuric acid was added to the substance, after which the resulting solution was made to the mark with the 10 N H_2SO_4 solution.

2.1.2. Preparation of hydrazine sulfate solution

0.375 g of hydrazine sulfate was weighed using an analytical balance and placed into a 250 mL volumetric flask and dissolved using distilled water. The solution was made up to the mark.

2.1.3. Preparation of the phosphate standard solutions

The stock solution was prepared by placing potassium dihydrogen phosphate containing 90% phosphate into a 1.0 L volumetric flask. Aliquots of the stock solution were then used to prepare a series of standard phosphate solutions in 25 mL volumetric flasks of concentrations: 10%, 25%, 45%, 50%, 60%, 70%, and 80%.

2.1.4 Preparation of standards and samples for phosphate quantitation and kinetic studies

To each of the prepared aliquots of the stock phosphate standard solutions, 5 mL of ammonium molybdate and 2 mL of hydrazine sulfate were added to the 25 mL volumetric flasks. The standards were left on the bench for about 3 hours to develop an intense blue color due to the formation of an ammonium hydrazine-phosphomolybdate (AHPM) complex. A blank solution contained an aqueous solution of the ammonium hydrazine-complex (with

no phosphate ions) placed in the reference beam for the analysis. Photometric measurements at λ = 820 nm were used to develop a calibration curve for the quantitative determination of percent phosphate levels.

Exactly 1.0 g of each of the finely ground fertilizer samples was digested using the perchloric acid digestion method after which the mixtures were filtered using Whatman filter paper. From the procedure, a suitable aliquot sample was transferred into 25 mL volumetric flasks and brought to the mark using distilled water. To each of the samples, a 2 mL mixture of 5 mL of ammonium molybdate and 2 mL of hydrazine sulfate was added and the solutions were shaken vigorously and allowed to stand for about 3 hours for a blue color to develop before being subjected to replicate photometric absorbance measurements at λmax.= 820 nm. The absorbance measurements were then converted to phosphate percent concentrations.

Kinetic studies to characterize the formation of ammonium hydrazine-molybdate complex (AHM) were conducted by preparing and reacting 1M ammonium molybdate with 1M hydrazine sulfate. In the case of studying the formation of the phospho-ammonium-hydrazine-molybdate complex (AHPM), 1.5 mL of the stock solution of phosphates was added to the 2 mL of the AHM complex solution.

2.2. Instrumentation

A UV-VIS K9000 double-beam spectrophotometer with a wavelength scan range in range between 190 – 1100 nm was used to conduct the kinetic and photometric experiments. The wavelength scans were also performed to analyze the variation in the absorption spectra of the complexation reactions. All the spectrophotometric measurements were recorded by placing the sample solutions in a cuvette of the path length of 1 cm and measured against a reference cell containing an appropriate solvent solution.

3. RESULTS AND DISCUSSION

The modified method of phosphate determination is based on the formation of ammonium hydrazine-phosphomolybdate complex that forms due to the reaction between ammonium molybdate, hydrazine, and phosphates to give the blue-colored complex for colorimetric analysis.

3.1 Spectroscopic study of the ammonium-molybdate (AM) Complex

In this section, a spectroscopic study into the formation of the ammonium hydrazine-molybdate complex is presented. To do this, wavelength scan measurements of the reactants are first conducted separately. In Figure 1, the absorption spectra of the solutions of ammonia, ammonium molybdate (in acid), and ammonium molybdate (without acid) are presented.

It can be observed that an aqueous solution of ammonia (NH_3) gives an intense absorption band in the UV region with a peak of $\lambda_{max.}$ = 201 nm. The NH_3 molecule contains loosely bound non-bonding electron pair and therefore one of the most probable electronic transitions contributing to the observed absorption band would be the *n to* σ* transitions. The spectrum in blue as derived from the solution of the ammonium molybdate (AM) complex in the absence of sulphuric acid gives a strong broad absorption band in the range of about 280 – 380 nm.

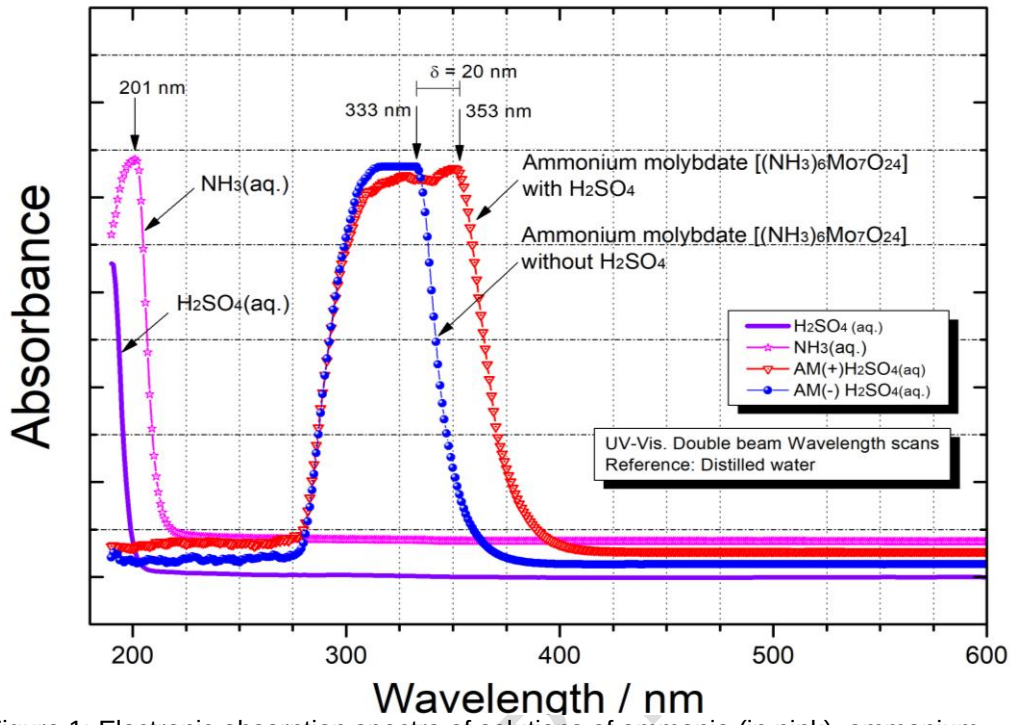

Figure 1: Electronic absorption spectra of solutions of ammonia (in pink), ammonium molybdate in acid (in red), and ammonia molybdate solution without acid (in blue)

The spectrum in red derived from the acidified ammonium molybdate solution shows a characteristic absorption band that is similar to that of the former spectrum except that it is broader. The spectra of the ammonium molybdate complexes all appear deep-orange in color and the broad, strong absorption bands most probably arise due to the characteristic intense charge-transfer electronic transitions commonly observed in metal-oxo complexes.[13] The difference in the full-width and half-maximum (FWHM) is about 20 nm as illustrated in the figure. Band broadening in the absorption spectra that occurs as a result of acidification with the mineral acid H_2SO_4 is a possible indication of the existence of binding of sulfate ions that creates a more disordered AM complex.[14]

3.2 Spectroscopic study of ammonium hydrazine-molybdate (AHM) complex formation

In this section, the wavelength scan measurements are conducted to probe the formation of the ammonium hydrazine-molybdate (AHM) complex. The complex formation results due to the reaction between the AM complex and the hydrazine sulfate solution

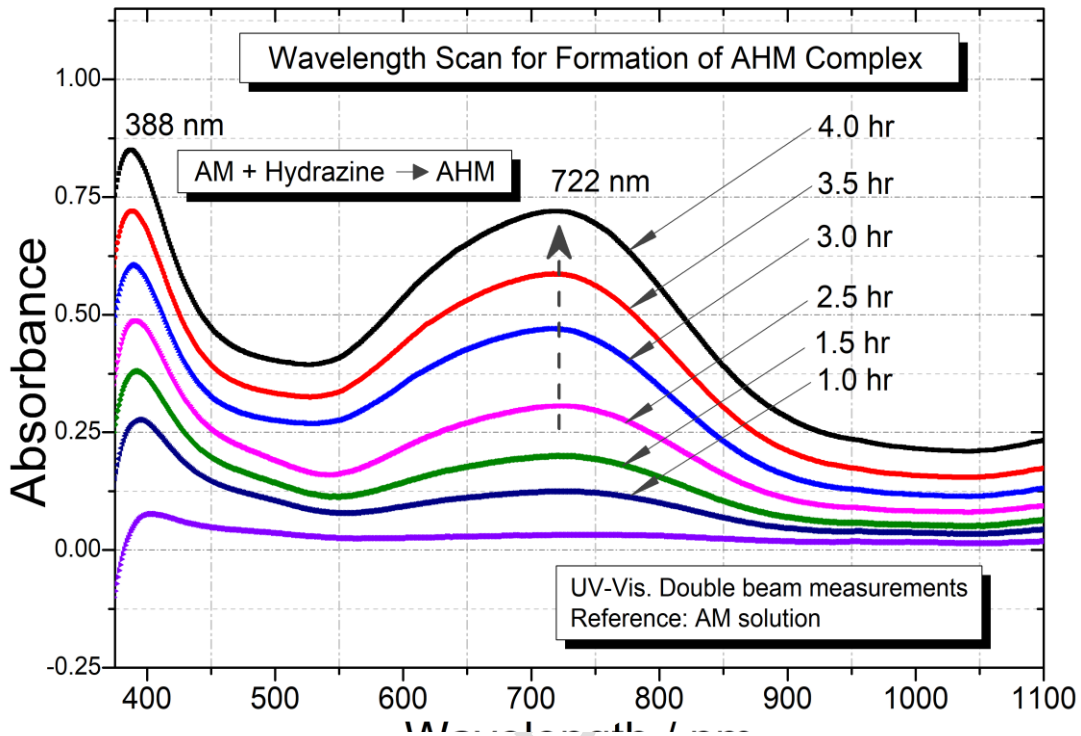

Figure 2: UV-Visible wavelength scan measurements investigating the formation of ammonium hydrazine-molybdate (AHM) complex

Figure 2 shows the time-dependent spectra obtained during the reaction monitoring experiment at 1-hour intervals for a total of 5 hours. From Figure 2, it can be observed that the AHM complex forms slowly at room temperature and exhibits a broad absorption in the visible range from about 550 nm to about 950 nm with $\lambda_{max.}$ at about 722 nm. The spectrum of hydrazine (in cyan color) is included as a reference and shows no absorption bands, which means that the absorption bands that develop over time are exclusively due to AHM complex formation.

3.2.1 Kinetic study of the formation of the AHM complex

Figure 3 illustrates the kinetic profile for the formation of the AHM complex. The graph was obtained from photometric measurements conducted at λ set at 722 nm for an extended reaction time of up to 4,200 s as informed by the results in Figure 2. The reference cell used during the measurement was a solution of AM to elucidate only the effect of hydrazine in its reaction with the AM complex as the absorbance values are recorded throughout the reaction time.

It is evident from Figure 3 that the absorbance values increase over time in the course of the complexation reaction. The gradient of the curve (synonymous with the reaction rates) is lower within the first 0 – 1,200 s relative to those over the extended reaction times (> 2000 s). This points to the appearance of more reaction mechanisms developing over the extended reaction times during the complexation reaction.

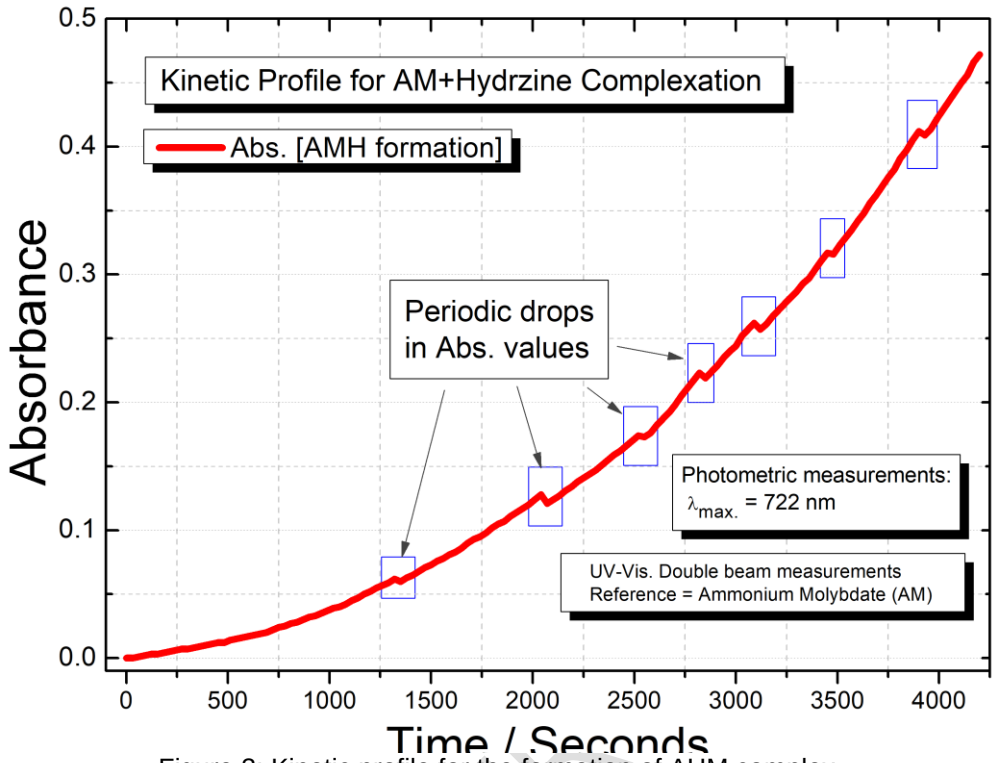

Figure 3: Kinetic profile for the formation of AHM complex

The periodic drops in absorbance values (or concentration) of the products as attested by the kinetic profile in Figure 3. This phenomenon progressively becomes more erratic, especially during the extended reaction time phase (for this case > 1,250 s – 4,200 s). These are possible indications of the dissociation mechanisms that would explain the temporary disappearances of product species (or complex dissociation events) evident at later stages of the complexation reaction. It can also be observed that the reaction successively increases in rate after the periodic drops in absorbance values. A possible indication of the successive or step-wise establishment of several chemical equilibria within the reaction system which is typical of complexation reactions.[15]

From the inset graph in Figure 4 (whose time axis is presented in the linear scale), it can be observed that in the initial phase (0 - 1000 s), when 2M Hydrazine is used (spectrum in red) the rate of reaction is faster than in the case where 1M Hydrazine is used (spectrum in blue).

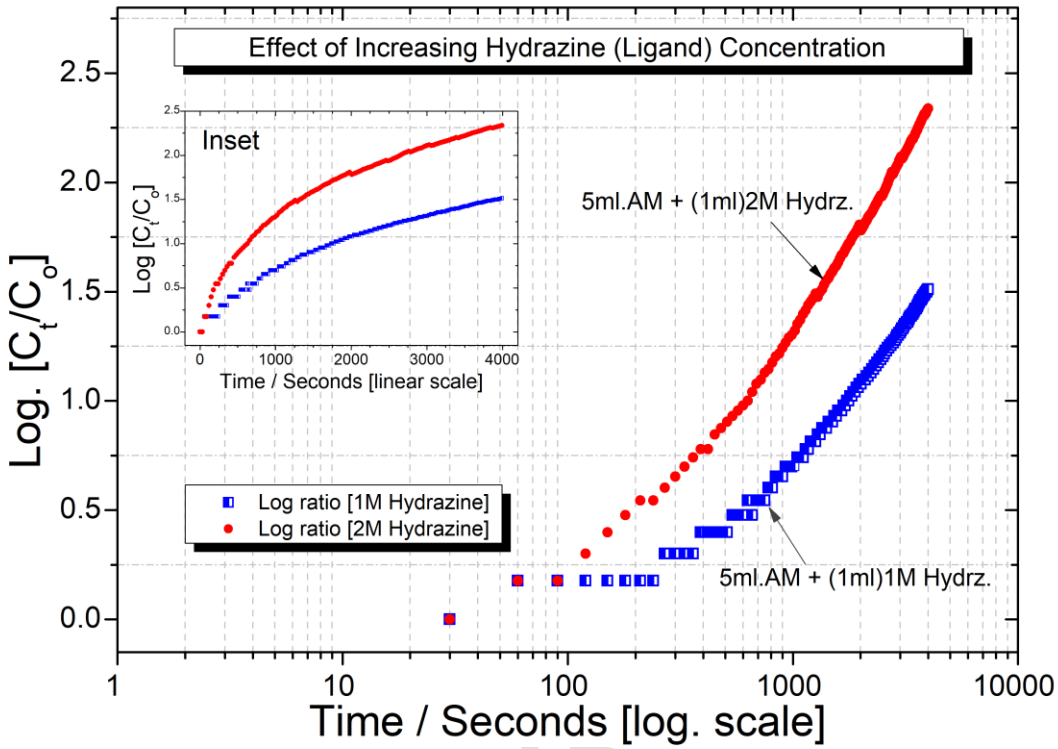

Figure 4: Effect of increasing hydrazine concentration on the rate of formation of AHM complex

In Figure 4 (both the linear and log scale plots) higher product concentration values (as depicted by the values of the C_t/C_o log ratios) are generally recorded in the case of 2M Hydrazine than in the case where 1M Hydrazine is used. This means that an increase in the ligand concentration enhances the rate of the complexation reaction as higher rate constants are observed when the concentration of the ligand is doubled. The log-scale graph of Figure 4 shows that there is a departure from around the 90th second where the reaction with 2M Hydrazine accelerates while that of 1M Hydrazine stagnates. It can also be noted that even though there is a trend of rising concentration in later phases of the reaction, the rate constants in both cases seem to be identical (i.e., from 2000 s onwards) as opposed to the trend observed in the initial phase from 0 – 1000 s. Because the reaction rates appear in a diminishing trend (as observed in the inset in Figure 7), it means that the system is moving towards chemical equilibrium as the reversible processes become more important in the later phases of the reaction.

3.2.2 Graphical fitted tests for the determination of the order of reaction for the formation of AHM complex

The data obtained from the kinetic profile in Figure 5 was used to determine the order of the reaction that leads to the formation of the AHM complex within the first 660 s. The kinetic analysis based on the integrated rate equation plots is displayed in Figure 5 (a-d) and labeled appropriately in the respective graphs. Figures 5 (a, b, and c), show the graphical fitted tests for zero-order, first-order, and second-order kinetics respectively based on the related integrated rate equations.

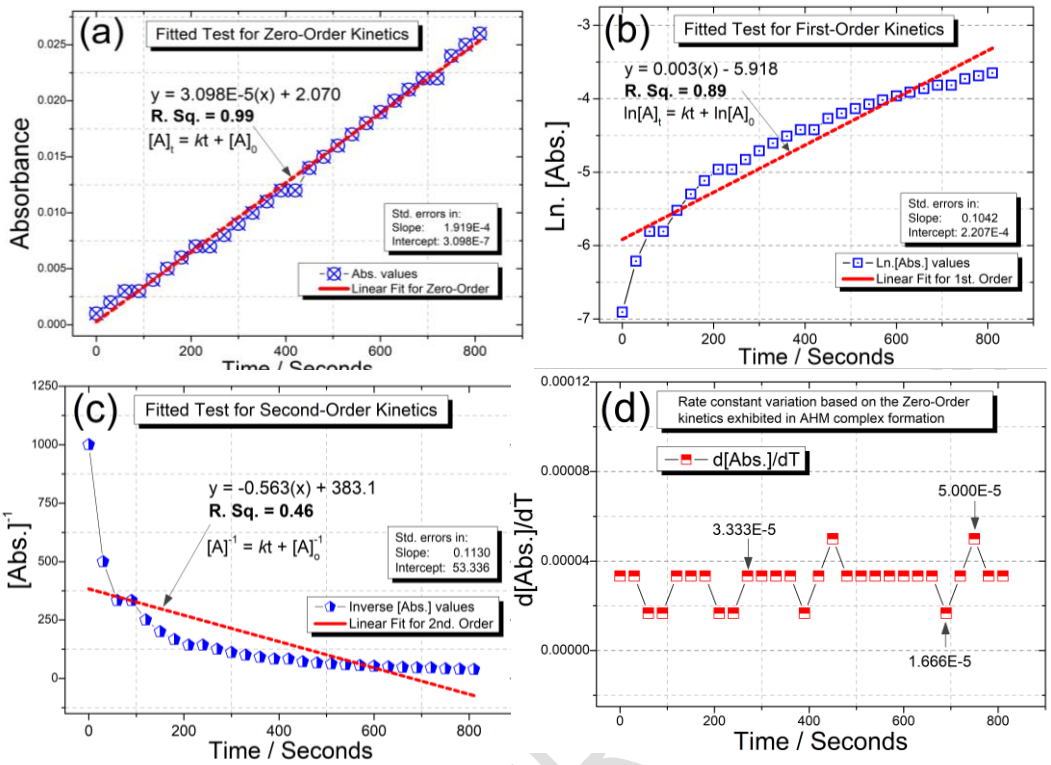

Figure 5 (a-d): Graphical kinetic analysis for the formation of AHM complex

From the graphical fitted test graphs in Figures 4(a, b and c). The absorbance versus time data best fits into a linear model (R^2 = 0.99) as opposed to the fitted tests in first- or second-order kinetics where the regression equation fits with lower R^2 values of 0.89 and 0.46 respectively. Moreover, the standard errors in the slope and intercept (as indicated in the graphs) for the linear fitted equations are lowest in the fitting test for zero-order kinetics as opposed to first- and second-order kinetic analyses. They are in the orders of magnitude of 10^{-4} and 10^{-7} respectively. This is a clear indication that the reaction that leads to the formation of the AHM complex follows zero-order kinetics. The gradient of the fitness test for zero-order kinetics in Figure 5(a), whose value is 3.089 x10^{-5} represents the average rate constant of the complexation reaction in the initial stages of the reaction. The rate constant variation is graphed in Figure 5(d) by plotting the computed derivatives (d[Abs.]/dT) as a function of time. The computed rate constants are in the neighborhood of 3.333 x 10^{-5} (+/-) 1.666x10^{-5} and remain frequently constant at the value of 3.333 x 10^{-5} from the onset of the reaction in the reaction phase under investigation.

3.3 Spectroscopic study of the formation of ammonium hydrazine-phopho-molybdate (AHPM) complex

Figure 6 contains spectra of the periodic wavelength scan measurements obtained during the reaction between AHM complex and phosphoric acid in solution studies over 2 hours. The measurements were made with the AHM complex solution as the reference to subtract its spectroscopic effect on the resultant spectra.

The formation of the phospho-complex (AHPM) is observed by the gradual increase in the intensity of maximum absorption detected at about 820 nm. It can be noted that the AHM complex (with no phosphates) gives a maximum absorbance at about 722 nm (Figure 2) in contrast to the AHPM complex (with phosphates).

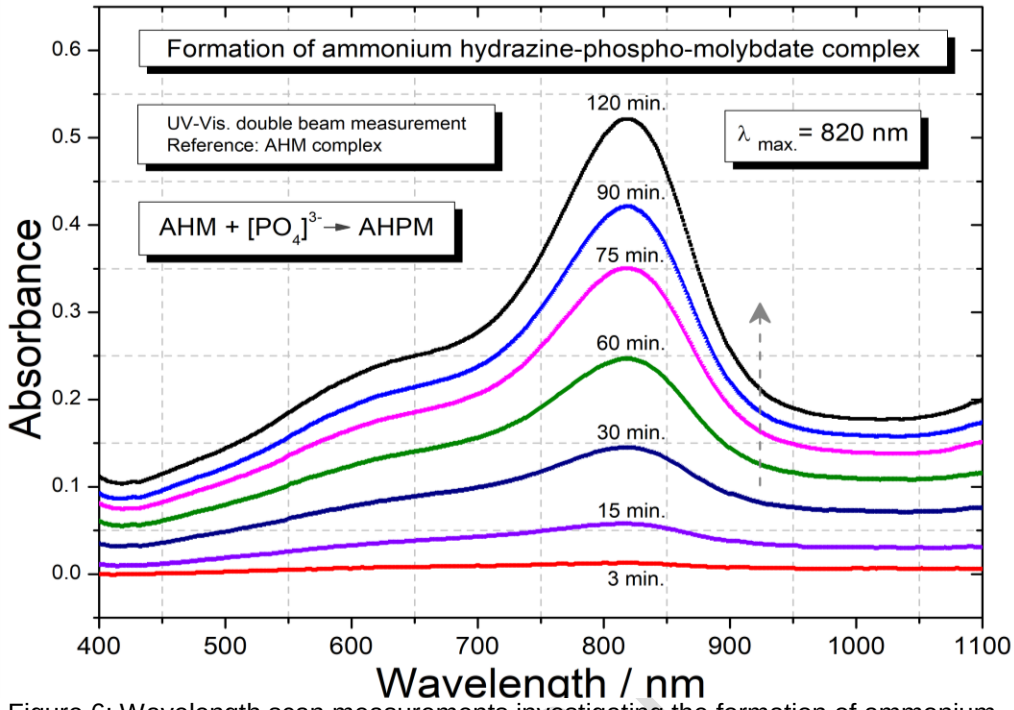

Figure 6: Wavelength scan measurements investigating the formation of ammonium hydrazine-phospho-molybdate (AHPM) complex

The $\lambda_{max.}$ value observed in this study is consistent with other previous studies.[11],[16] The UV-Visible wavelength scan measurements show that appreciable amounts of the product can be detected as early as the first 15 mins. The reaction solution turns from greenish-blue to more intense blue coloration, which characterizes the formation of the phospho-molybdate complex (AHPM). Another absorption band with smaller intensity is observed in the range of 550 – 660 nm. This appears as a shoulder peak to the maximum absorption band at 820 nm and tends to become more prominent at the latter stage of the reaction (> 60 min).

3.3.1 Kinetic study of the formation of AHPM complex

Figure 7 shows the kinetic measurements conducted photometrically by monitoring the maximum absorption wavelength of 820 nm for about 42 minutes during the reaction. The reference in the double beam measurement was the AHM complex that contains no phosphates. The kinetic profile reveals a rise in absorbance values due to the formation of the AHPM complex, whose maximum absorption occurs at about 820 nm. It should be noted that the influence of the AHM complexation is removed by the reference in the measurement, only the reaction due to the formation of the phospho-complex contributes to the rise in the absorbance values.

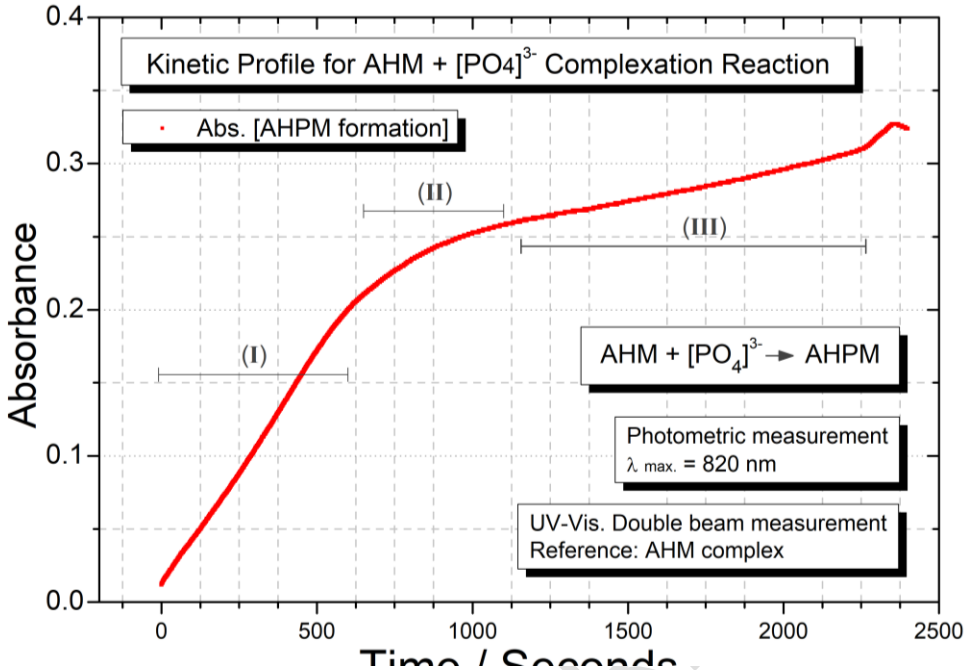

Figure 7: Kinetic profile for the formation of ammonium hydrazine-phospho-molybdate (AHPM) complex

It can be observed that the rate of the reaction changes a bit drastically in about three phases during the reaction as indicated by the sub-divisions I, II, and II in Figure 7. Phases I and II appear linear while phase II is not linear. This means that the kinetic profile for the reaction monitored generally depicts a mixed-order reaction within the reaction period investigated. Of the three phases, phase I has the highest average rate constant. This means that the rate of formation of the phospho-complex is highest in phase I from the onset of the reaction. Although there is a general rise in absorbance values, phases II and II have lower average rate constants, a possible indication of depletion of the phosphates that drive phase I and perhaps other complex mechanisms that take route in the later phases.

3.3.2 Graphical fitted tests to determine the order of reaction in the formation of AHPM complex

Figures 8(a, b, c, and d) illustrate the kinetic analysis performed to determine the order of the reaction that leads to the formation of the AHPM complex and the rate constant. The graphs are derived from the analysis of experimental data derived from the kinetic profile shown earlier in Figure 8 (section 3.3.1) selected within the first 600 s.

From the kinetic analyses in Figure 8(a, b and c), which are summarized in table 1, it is clear that the graphical fitted test for zero-order kinetics gives the highest r^2 value of 0.99, while the fitted tests for first- and second-order have lower R.Sq. values of 0.91 and 0.63 respectively.

Table 1: Determination of order of the complexation reaction between ammonium-hydrazine molybdate and phosphates

Test	Equation	R.Sq. Value
Zero-Order	$y = 3.195x10^{-4}(x) + 0.010$	0.999
First-Order	$y = 0.003x10^{-4}(x) - 3.557$	0.909

Second-Order	$y = -0.626x10^{-4}(x) + 33.327$	0.629

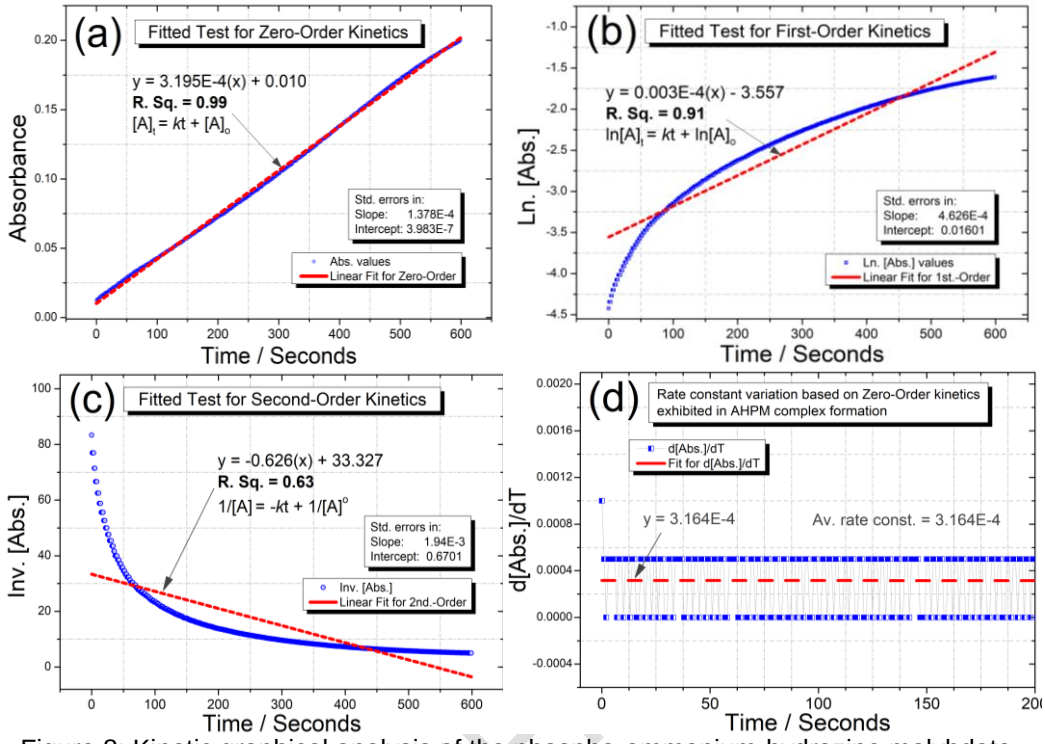

Figure 8: Kinetic graphical analysis of the phospho-ammonium-hydrazine molybdate complexation reaction

The fitting in the graph of absorbance (or concentration) versus time is linear with a slope of 3.195×10^{-4} and has the lowest standard errors in the orders of 1.378×10^{-4} and 3.983×10^{-4} for the slope and intercept respectively. This proves that the complexation reaction follows zero-order kinetics. Figure 8(d), illustrates the variation of rate constants computed by plotting the instantaneous rate values (d[Abs.]/dT) over the reaction period of between 0 – 200 s and the computed average rate constant value of 3.164×10^{-4} $M.s^{-1}$.

3.4 Spectrophotometric determination of phosphate levels in selected fertilizers

3.4.1 Wavelength scan absorption spectra of the phosphate standards and calibration curve

Figure 9 shows the absorption spectra obtained from the wavelength scans of the phosphate standards. The standards were freshly prepared and the scans were conducted to inspect a linear correlation of the absorbance within the percent phosphate concentration range prepared. The measurements were conducted 1 hour after fresh preparations of the standards were made against the ammonium-hydrazine-molybdate reference solution.

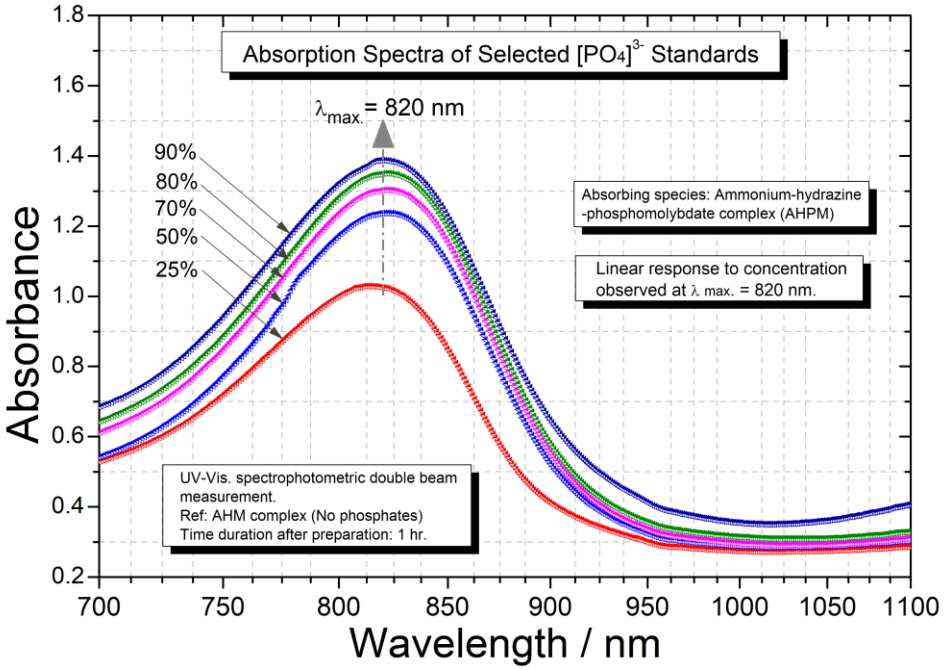

Figure 9: Absorption spectra of selected phosphate standards

As evident in Figure 9, the absorption maximum absorption of the phospho-complex AHPM occurs at about 820 nm. As expected, the maximum absorption intensity of the phosphate - standards rises with increasing phosphate–standard concentrations.

Figure 10 shows the calibration curve developed by plotting the mean absorbance values of the standards for the determination of phosphate levels based on the photometric measurements conducted in triplicate at 820 nm. The *Beer-Lambert* equation is obeyed within the concentration range investigated (R^2 = 0.99).

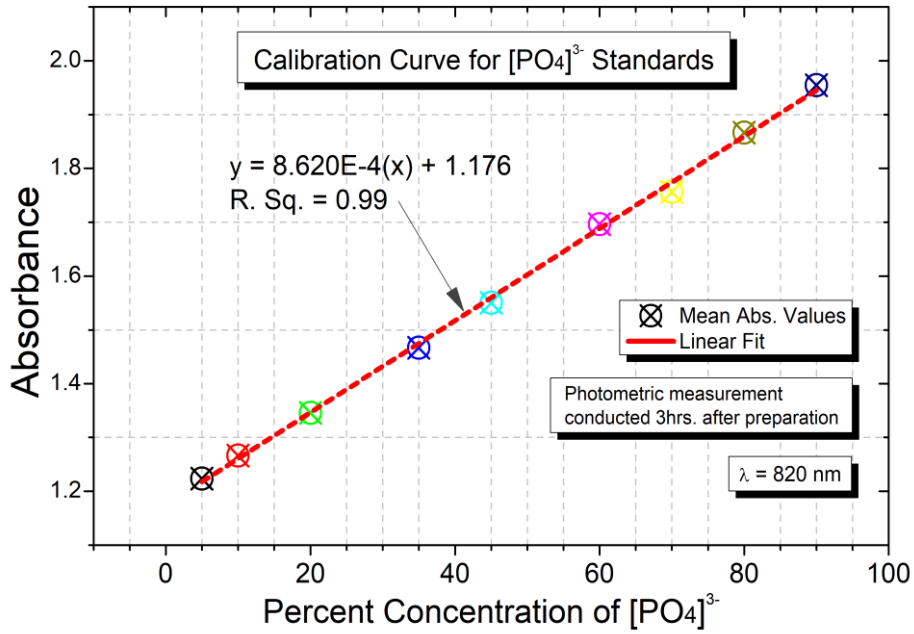

Figure 10: Calibration curve developed based on absorbances of phosphate standards

The predictor equation for concentration as derived from the linear fit is Abs. = 8.62 x 10^{-4} (Conc./%) + 1.176. The absorption measurements for the calibration plot were conducted 24 hrs. after the preparation of the standards. The standard errors in the intercept and intercept are 0.00662 and 1.311 x 10^{-4} respectively, which are very low.

3.4.2 Determination of phosphate levels in the commercial fertilizers

Table 2 shows the data obtained in the spectrophotometric determination of phosphate levels in the selected commercially available samples. The commercial fertilizer samples were classified into two groups; organic and inorganic based. The absorbance values were experimentally obtained from the triplicate measurements at 820 nm for each of the samples and converted to percent concentrations using the regression equation derived from the calibration plot in Figure 10. The mean and standard deviation values for each set of the triplicate experiments are also tabulated.

Table 2: Determination of percent phosphate concentrations in the fertilizer samples

		Experimental Abs. Values			**Calculated $[PO_4]^{3-}$ Concentrations (%)**			**Av. $[PO_4]^{3-}$ Conc. (%)**	**SDEV. (+/-)**
		Abs. 1	Abs. 2	Abs. 3	Conc. 1 (%)	Conc. 2 (%)	Conc. 3 (%)		
Inorganic	S1	1.811	1.821	1.819	73.666	74.826	74.594	74.36	0.61
Fertilizers	S2	1.801	1.806	1.802	72.506	73.086	72.622	72.74	0.31
	S3	1.847	1.842	1.841	77.842	77.262	77.146	77.42	0.37
	S4	1.717	1.708	1.733	62.761	61.717	64.617	63.03	1.47
	S5	1.719	1.711	1.709	62.993	62.065	61.833	62.30	0.61
	S6	1.891	1.898	1.891	82.947	83.759	82.947	83.22	0.47
	S7	1.819	1.908	1.828	74.594	84.919	75.638	78.38	5.68
	S8	1.754	1.798	1.761	67.053	72.158	67.865	69.03	2.74
	S9	1.827	1.818	1.831	75.522	74.478	75.986	75.33	0.77
							Mean (+/-) SDEV. =	**72.87**	**6.98**
Organic	S10	1.662	1.678	1.683	56.381	58.237	58.817	57.81	1.27
Fertilizers	S11	1.621	1.608	1.624	51.624	50.116	51.972	51.24	0.99
	S12	1.697	1.698	1.694	60.441	60.557	60.093	60.36	0.24
	S13	1.609	1.604	1.611	50.232	49.652	50.476	50.12	0.42
	S14	1.544	1.548	1.554	42.691	43.155	43.852	43.23	0.58
							Mean (+/-) SDEV. =	**52.55**	**6.77**
Unpaired *t*-Test (Between means of the two groups)							*p*-value at 95% CI =	0.001	< 0.05

It was found that the percent phosphate content among the inorganic fertilizers was found to range between 61.7% - 82%. Whereas in the organic fertilizer samples investigated, the range was between 43.8 % - 58.2%. An unpaired t-test reveals that the mean percent concentrations between the two groups of fertilizer samples tested are significantly different since the *P*-value of 0.001 is less than 0.05.

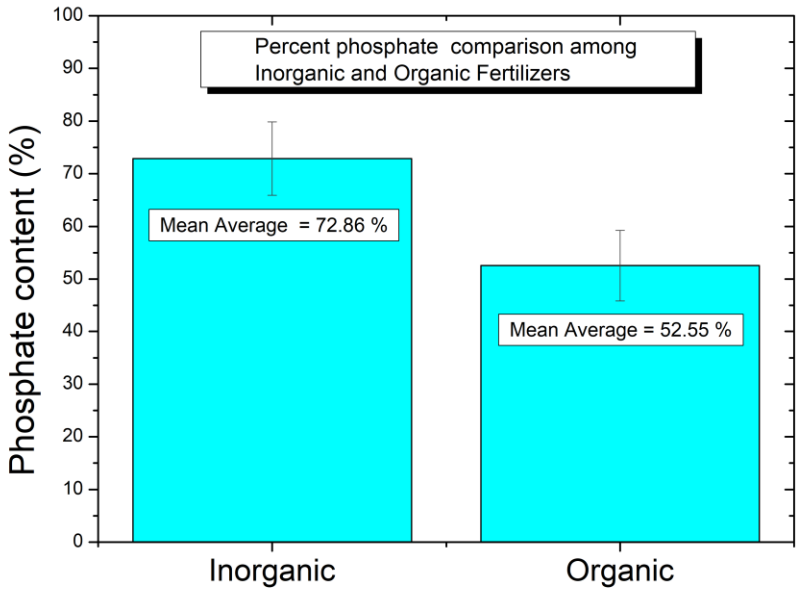

Figure 11: Comparison of the phosphate levels between the inorganic and organic commercial fertilizer samples investigated

The results in table 1 are further summarized in the simple histogram chart in Figure 11 which shows a comparison of the levels of percent phosphates in inorganic versus organic commercially available fertilizers. The mean average phosphate content in the inorganic fertilizers was found to be higher (at 72.8%) than in the organic fertilizers (at 52.5%). This means that the quantity of detectable phosphates in inorganic fertilizers is generally higher than in organic fertilizers.

Typical organic fertilizers include all types of animal waste including meat processing waste, manure, and slurry, plus plant-based fertilizers such as compost; and biosolids. Inorganic fertilizers include minerals such as rock-phosphate and ash materials. Organic fertilizer generally requires a considerable amount of time for the contents to be broken down by microorganisms to be readily available for plant uptake. Inorganic fertilizers, on the contrary, contain nutrients that can be readily absorbed by plants. This is perhaps a contributing factor as to why they're more phosphate detectable in them as opposed to the organic fertilizers investigated.

4. CONCLUSION

The experimental studies on the rates of formation of the molybdenum complexes with hydrazine and phosphates were successfully investigated. The binding of phosphates was successfully characterized by monitoring the formation of the ammonium-hydrazine-phospho-molybdate (AHPM) complex, whose maximum absorption was 820 nm. It was also shown that increase in hydrazine ligand concentration has an accelerating effect on the rate of formation of the ammonium-hydrazine-molybdate (AHM) complex whose maximum absorption was 720 nm. The kinetic investigations on the formation of both AHM and AHPM complexes revealed that the reactions proceed via zero-order kinetics overall.

The formation of the AHPM complex was able to elucidate the spectrophotometric determination of percent phosphate content in selected commercially available fertilizer samples. This is because their color intensity was found to be proportional to the concentration of the standards at R^2=0.99. This validated the simple spectrophotometric analytical method. The experimental elucidation of the complexation reactions using UV-

Visible spectroscopy adds to the fundamental knowledge in understanding the mechanisms involved and is exploited in many other spectrophotometric analytical techniques. The quantification of phosphates revealed that approximately a third of the inorganic fertilizers tested had slightly lower phosphorus levels than the recommended limit. It was also found that the inorganic fertilizers tested had significantly higher phosphorus content than those contained in the organic fertilizers in the market.

REFERENCES

[1] T.L. Roberts, A.E. Johnston, Phosphorus use efficiency and management in agriculture, Resour. Conserv. Recycl. 105 (2015) 275–281. https://doi.org/10.1016/j.resconrec.2015.09.013.

[2] N.C.M. Pereira, F.S. Galindo, R.P.D. Gazola, E. Dupas, P.A.L. Rosa, E.S. Mortinho, M.C.M.T. Filho, Corn Yield and Phosphorus Use Efficiency Response to Phosphorus Rates Associated With Plant Growth Promoting Bacteria, Front. Environ. Sci. 8 (2020) 1–12. https://doi.org/10.3389/fenvs.2020.00040.

[3] C. Alewell, B. Ringeval, C. Ballabio, D.A. Robinson, P. Panagos, P. Borrelli, Global phosphorus shortage will be aggravated by soil erosion, Nat. Commun. 11 (2020). https://doi.org/10.1038/s41467-020-18326-7.

[4] A. Pal, R. Adhikary, Improving of Phosphorus use Efficiency in Acid & Alkaline Soil : a Critical Review Study Improving of Phosphorus use Efficiency in Acid & Alkaline Soil : a, Indian J. Nat. Sci. 10 (2020) 18558–18562.

[5] O. Topcu, C; Coldur, F; Caglar, B; Volkan Odzokur, K; Cubuk, Solid-state Electrochemical Sensor Based on a Cross-linked Copper(II)-doped Copolymer and Carbon Nanotube Material for Selective and Sensitive Detection of Monohydrogen Phosphate, Electroanalysis. 13 (2022) 474–484.

[6] K. Grudpan, P. Ampan, Y. Udnan, S. Jayasvati, S. Lapanantnoppakhun, J. Jakmunee, G.D. Christian, J. Ruzicka, Stopped-flow injection simultaneous determination of phosphate and silicate using molybdenum blue, Talanta. 58 (2002) 1319–1326. https://doi.org/10.1016/S0039-9140(02)00441-1.

[7] E.A. Nagul, I.D. McKelvie, P. Worsfold, S.D. Kolev, The molybdenum blue reaction for the determination of orthophosphate revisited: Opening the black box, Anal. Chim. Acta. 890 (2015) 60–82. https://doi.org/10.1016/j.aca.2015.07.030.

[8] K.M. Giannoulis, G.Z. Tsogas, D.L. Giokas, A.G. Vlessidis, Dispersive micro-solid phase extraction of ortho-phosphate ions onto magnetite nanoparticles and determination as its molybdenum blue complex, Talanta. 99 (2012) 62–68. https://doi.org/10.1016/j.talanta.2012.05.021.

[9] S. Ganesh, F. Khan, M.K. Ahmed, P. Velavendan, N.K. Pandey, U. Kamachi Mudali, Spectrophotometric determination of trace amounts of phosphate in water and soil, Water Sci. Technol. 66 (2012) 2653–2658. https://doi.org/10.2166/wst.2012.468.

[10] F.E. Adelowo, S.O. Agele, Spectrophotometric analysis of phosphate concentration in agricultural soil samples and water samples using molybdenum blue method, Brazilian J. Biol. Sci. 3 (2016) 407–412. https://doi.org/10.21472/bjbs.030616.

[11] S. Pradhan, M.R. Pokhrel, Spectrophotometric Determination of Phosphate in Sugarcane Juice , Fertilizer , Detergent and Water, Sci. World. 11 (2013) 58–62.

[12] C.X. Galhardo, J.C. Masini, Spectrophotometric determination of phosphate and silicate by sequential injection using molybdenum blue chemistry, Anal. Chim. Acta. 417 (2000) 191–200. https://doi.org/10.1016/S0003-2670(00)00933-8.

[13] S.A. Khan, Charge-Transfer Complexes: A Short Review, J. Emerg. Technol. Innov. Res. 1 (2014) 52–58.

[14] F. Zsila, Z. Bikadi, M. Simonyi, Probing the binding of the Flavonoid, quercetin to human serum albumin by circular dichroism, electronic absorption spectroscopy and molecular modelling methods, Biochem. Pharmacol. 65 (2003) 447–456.

[15] P. Ryan, M.J. Hynes, The kinetics and mechanisms of the complex formation and antioxidant behaviour of the polyphenols EGCg and ECG with iron (III), J. Inorg. Biochem. 101 (2007) 585–593. https://doi.org/10.1016/j.jinorgbio.2006.12.001.

[16] X.L. Huang, J.Z. Zhang, Kinetic spectrophotometric determination of submicromolar orthophosphate by molybdate reduction, Microchem. J. 89 (2008) 58–71. https://doi.org/10.1016/j.microc.2007.12.001.